PCA-Based Classification for 3D Ultrasonic Reflectors

A. Ochoa, J. Ureña, A. Hernández, M. Mazo, J.A. Jiménez, M.C. Pérez
University of Alcala/Electronics Department, E-28806 Alcala de Henares (Madrid), Spain
E-mail: {alberto, urena, alvaro, mazo, jimenez, carmen}@depeca.uah.es

Abstract. — **In this work a classification system for basic ultrasonic reflectors (plane, corner and edge) in three-dimensional (3D) environments is presented. The classification system is based on the principal component analysis (PCA) technique and the times-of-flight (TOF) are used as classification parameter. The system provides a sensorial structure to simultaneously obtain up to 16 TOF in every emission/scanning process. With the set of obtained TOF, it is possible to identify the ultrasonic reflector, as well as its position and range in 3D environments. The results achieved by the classification system are satisfactory, since the three reflector types are identified and located in 3D environments.**

Keywords – **Classification system, PCA, TOF, ultrasonic reflectors.**

I. Introduction

Classification systems applied to ultrasonic environments are continuously modified in theirs different stages, with the purpose of increasing the percentage of success in reflector classification. These improvements allow the possibility of identifying different reflector types in three-dimensional (3-D) environments. The main changes in these classification systems are sensorial structure, low-level processing techniques, and algorithms used for classification. With these modifications, the sensor system can provide more information from 3D environments in less time.

Sensorial structures used in these classification systems often present different number of ultrasonic transducers and geometric configurations [1][2]. The Times-of-Flight (TOF) and amplitudes extracted from echoes captured by the sensor can be used as classification parameters in reflector recognition algorithms [2][3]. The extraction of these parameters can be carried out by different techniques applied to signals captured by the sensorial structure [4]. It is possible to find the use of encoding techniques with some sequences to simultaneously transmit with several transducers (pseudo-random [5], complementary sequences [6], etc.). These encoding techniques also allows to determine TOFs with more accuracy, by applying correlation techniques.

Different models of sensorial structures have been used for object classification in two-dimensions (2-D) [2] and three-dimensions (3-D) [7]. The three basic reflectors, more usual in 2-D environments, are plane, edge and corner [1]. The reflector classification is important since it can be used in mapping tasks for indoor environments and in localization of mobile robots.

The PCA technique (Principal Component Analysis) has been used to reduce the dimension of data sets and object recognition in different works [8]. This technique can be applied in different fields, such as recognition of faces, sonar signal classification, object detection, and estimation of object position in 3-D [9].

In this work a classification system based on PCA technique is presented, for the identification of three-dimensional (3-D) ultrasonic reflectors. This system provides a sensorial structure that can extract information in a 3-D environment. The sensorial structure is formed by four transducers, which simultaneously emit a particular and different encoded signal assigned to every transducer. Simultaneously, at every receiver, echoes are detected and processed to obtain their corresponding TOFs. With the described system, up to 16 TOF can be simultaneously obtained in every scanning process. The TOFs are analyzed with the PCA technique in order to identify the ultrasonic reflector generating echoes. In addition, the system allows to obtain information about reflector location (range, azimuth and elevation).

The work is organized as follows: in Section II the developed sensorial structure is introduced, as well as the discretization of its frontal space; Section III is dedicated to analyze the classification algorithm based on PCA technique; in Section IV, some classification results are provided and; finally in Section V some conclusions are discussed.

II. Sensorial Structure

The proposed sensorial structure presented in Figure 1 has been developed to extract information in a 3-D environment and, subsequently, to classify ultrasonic reflectors with the obtained data.

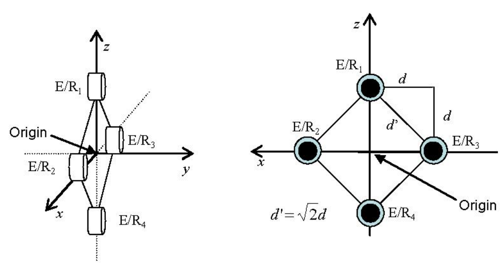

Figure 1. Developed sensorial structure (4 emitters/receivers).

The physical structure of the ultrasonic sensor consists of four transducers, all of them working as emitters and as receivers. The transducers in the sensorial structure are denoted as E/R$_i$, where $i \in \{1,2,3,4\}$. All the transducers are located in the plane x-z, with the axial axis in the y direction. Furthermore, the separation between transducers can be determined by the distance d (d=0.1m).

The four transducers can simultaneously emit a different encoded signal assigned to every emitter [6]. Moreover, the four transducers of the sensorial structure provide enough information to discriminate among the 3-D basic reflectors (plane, edge and corner) through the captured signals.

With four simultaneous emissions and receptions, up to 16 impulsive responses ($h_{i,j}$) $\{i,j=1,2,3,4\}$ are implied in the scanning process; where the emitter and the receiver are referred as i and j, respectively. In that way, up to 16 TOFs from the captured signals (echoes) can be measured. As example, in Figure 2 only the physical transmission channels among the emitter E/R$_1$ and the four receivers are shown. Every $h_{i,j}$ represented in Figure 2 may contain the principal echo and the multiple echoes coming from the reflector.

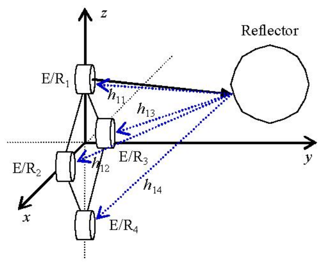

Figure 2. Configuration of the physical transmission channels for the emission of E/R$_1$.

The sensorial structure is formed by a horizontal vector sensor (E/R$_2$-E/R$_3$) and a vertical vector sensor (E/R$_1$-E/R$_4$), which allow to obtain information in both axes [9]. If the distance d among transducers is very small compared to the distance r between a reflector and the sensorial structure (d<<r), the problem of echo correspondence is reduced [4]. Because of the fact that the distance among transducers is small enough compared to the distance between the reflector and sensor, only one direction map is considered for the sensor. In other words, the emission–reception pattern of all transducers is centered in the coordinate origin of the sensor. This consideration is applied to any reflector with independence of its separation from the sensor. The reflector position in the 3D space can be determined from the set of TOFs provided by all the transducers. The reflector position in 3D is given by their spherical coordinates ($\vec{r}$ vector director, γ azimuth and θ elevation) or their cartesian coordinates (x, y, z); as observed in Figure 3.

The possible locations of reflectors in front of the sensorial structure in a 3-D space have been discretized. A perception zone model of the sensorial structure is created by discretizing the frontal space to build a map of directions and position.

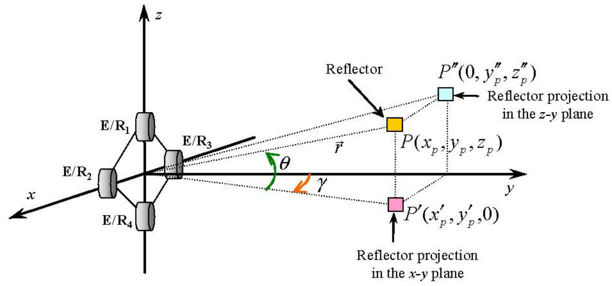

Figure 3. Spatial localization of a reflector in front of the sensor.

Every position of the map involves a distance r and two angles (γ and θ). In Figure 4 the map of directions obtained by discretizing the frontal space is shown; this space has an aperture angle in azimuth of ±45° with $\Delta\gamma$=5.6°; and in elevation of ±40.5° with $\Delta\theta$=10.125°.

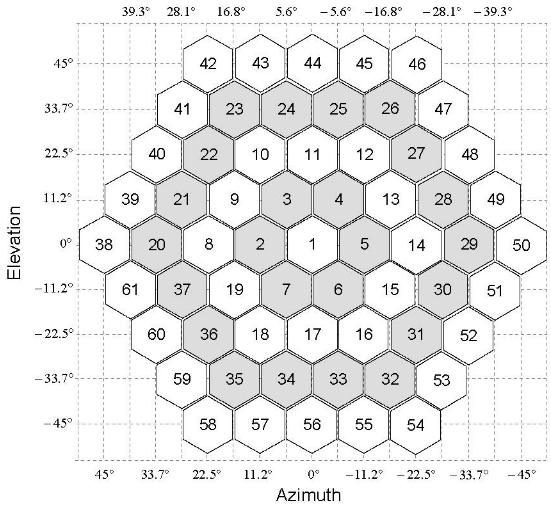

Figure 4. The direction map of the perception zone.

In Table I the distribution of positions in every ring (hexagon) of the direction map and its respective aperture in azimuth and elevation is summarized. The advantage of this configuration in hexagons is that this map can be adapted to the different emission-reception patterns of the ultrasonic transducers. For example, if the transducer has an aperture angle of ±30°, the map will be only formed by the first 4 concentric hexagons.

TABLE I.
Direction distribution and aperture angle at every concentric hexagon.

Hexagon	Positions in the map	Elements by hexagon	Aperture in azimuth	Aperture in elevation
1	1	1	0°	0°
2	2-7	6	±11.2°	±10.12°
3	8-19	12	±22.5°	±20.25°
4	20-37	18	±33.7°	±30.38°
5	38-61	24	±45°	±40.5°

The map of directions is centered in the coordinate origin of the sensorial structure as is shown in Figure 5. Every point of the map has as parameters: an r distance, γ elevation and θ azimuth angles; all of them represented by the $\vec{r}$ position vector. Moreover, it is possible to consider that every position of the direction map is located in the surface of a sphere. This is doable because the distance between the coordinate origin and every 3D position of the map is equal to r.

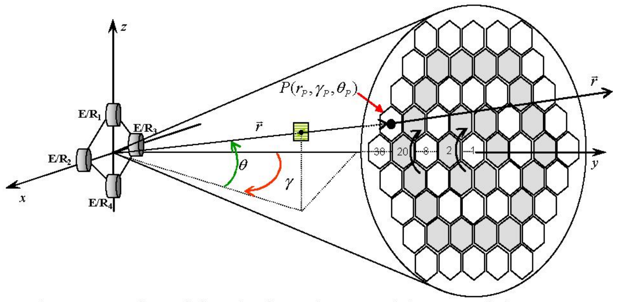

Figure 5. Discretizing the frontal space of the sensorial structure.

A. *Low level process*

An important characteristic of the proposed sensorial system is the possibility of carrying out a simultaneous emission with all the transducers. This is possible because every transducer has a macro-sequence assigned to codify its emission. Every binary macro-sequence is constructed from a Complementary Set of M Sequences (M-CSS) by interleaving each one of theirs bits. A set of M-CSS of length L_{sq} can be generated using an *Efficient Set of Sequences Generator* (ESSG) and, in the same form, an *Efficient Set of Sequences Correlator* (ESSC) can be implemented [6]. This new sequence constructed can be emitted with an ultrasonic transducer by a simple BPSK modulation. The echoes received by this transducer are processed in the reception stage to obtain the classification parameters. At every receiver, echoes are demodulated and correlated to identify each one of the transmitted macro-sequences.

In Figure 6 the block diagram of low-level processing applied to every transducer of the sensorial structure is shown. These low-level techniques allow TOFs from the received echoes to be obtained with more accuracy. In this case, if the sensorial structure simultaneously emits four different macro-sequences, in every transducer E/R_i four TOF can be obtained from the echoes processed. In example, in the Figure 6 is shown the detection of the MS_4 received by E/R$_i$ through its auto-correlation function, and subsequently to obtain the TOF$_{4,i}$ of this macro-sequence.

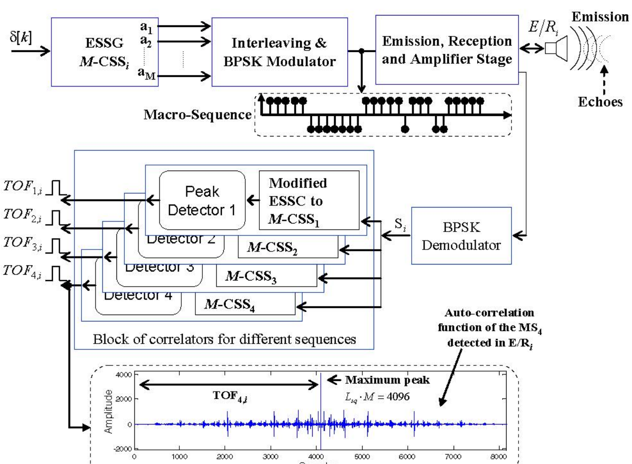

Figure 6. Block diagram of the processing carried out at every transducer.

III. Classification Algorithm Based on PCA

A. *Previous Considerations*

The PCA technique has been often used in areas of pattern recognition and computer vision, for data reduction and classification. In this work, PCA technique is used to carry out a classification of ultrasonic reflectors in 3D environments. The classification parameters used in this system are the TOF obtained with the sensorial structure shown in previous Section. The sensorial system allows to obtain up to N TOFs (N=16) due to the possibility of simultaneous emission with all the transducers of the sensor. This set of N TOFs forms a N-dimensional column vector identified by $\boldsymbol{\tau}$.

$$\boldsymbol{\tau} = [t_1 \quad t_2 \quad \cdots \quad t_N]^T \tag{1}$$

Where t_n is the TOF obtained by the sensorial system for the received echo, $n \in \{1, 2, \ldots, N\}$; and the super index T means transposed. If a training set of G TOFs vectors $\{\boldsymbol{\tau}_1, \boldsymbol{\tau}_2, \ldots, \boldsymbol{\tau}_G\}$ is considered taking values in a N-dimensional space, the average of TOF vectors of the set is defined by:

$$\boldsymbol{\Psi} = \frac{1}{G}\sum_{g=1}^{G}\boldsymbol{\tau}_g \tag{2}$$

Where $\boldsymbol{\Psi} \in \Re^N$. The difference $\boldsymbol{\Phi}_g$ between every TOF vector $\boldsymbol{\tau}_g$ and the average $\boldsymbol{\Psi}$ is obtained as:

$$\boldsymbol{\Phi}_g = \boldsymbol{\tau}_g - \boldsymbol{\Psi}, \quad g = 1,2,3,\ldots,G \tag{3}$$

Considering a linear transformation of the original N-dimensional vector of TOFs into a K-dimensional space, where $K \le N$, the new vector of characteristics $\boldsymbol{\rho}_g \in \Re^K$ is defined by the following linear transformation:

$$\boldsymbol{\rho}_g = \mathbf{U}_{opt}^T \cdot \boldsymbol{\Phi}_g \tag{4}$$

Where $\mathbf{U}_{opt}$ is the optimal transformation matrix, $\mathbf{U} \in \Re^{KxN}$. In order to obtain this matrix, it is necessary to compute the scattering matrix $\mathbf{C}$, defined by:

$$\mathbf{C} = \frac{1}{N}\boldsymbol{\Phi} \cdot \boldsymbol{\Phi}^T \tag{5}$$

To achieve the optimal transformation matrix $\mathbf{U}_{opt}$, the determinant of matrix $\mathbf{C}$ should be maximum:

$$\mathbf{U}_{opt} = \arg\max\left|\mathbf{U}^T\mathbf{C}\mathbf{U}\right| = [\mathbf{u}_1\mathbf{u}_2\cdots\mathbf{u}_K], \quad \forall K \le N \tag{6}$$

Where $\{\mathbf{u}_1, \mathbf{u}_2, \ldots, \mathbf{u}_K\}$ is the set of eigenvectors of $\mathbf{C}$ corresponding to the K largest eigenvalues $\{u_1, u_2, \ldots, u_K\}$. According to (4), the new sample-vector $\boldsymbol{\tau}_s$ in the transformed space is given by:

$$\boldsymbol{\rho}_s = \mathbf{U}_{opt}^T \cdot \boldsymbol{\Phi}_s = \mathbf{U}_{opt}^T(\boldsymbol{\tau}_s - \boldsymbol{\Psi}) \tag{7}$$

The reconstruction of $\boldsymbol{\Phi}_s$ from the transformed space, referred as $\boldsymbol{\Omega}_s$, is carried out though the inverse transformation given by:

$$\boldsymbol{\Omega}_s = \mathbf{U}_{opt} \cdot \boldsymbol{\rho}_s \tag{8}$$

The Euclidean distance (recovery error ε_s) between the characteristic vector of the recovered object $\mathbf{\Omega}_s$ and the sample $\mathbf{\Phi}_s$ is obtained by:

$$\varepsilon_s = \left\| \mathbf{\Phi}_s - \mathbf{\Omega}_s \right\| \tag{9}$$

With regard to the classification, if the recovery error is smaller than a threshold ($\varepsilon_s < E_S$), this sample has a great similarity with some element of the G-TOF vectors used to obtain the optimal transformation matrix $\mathbf{U}_{opt}$.

B. Reflector types

In the classification process carried out in this work, only three ultrasonic reflector types were considered assuming a 3D environment. These three reflectors (plane, corner, and edge) are defined by the $\vec{r}$ position vector shown in Figure 7. The edge-type reflector is represented by an ultrasonic specific scatter located at the reflection point $P(x_P, y_P, z_P)$. The plane-type reflector is defined by its position vector $\vec{r}$ and the point P, being $\vec{r}$ the normal line to the plane π. A corner-type reflector is formed by two planes intersected with an angle of 90°, observed from the concave side. The position vector $\vec{r}$ of a corner is defined to be normal to the interception line of the planes.

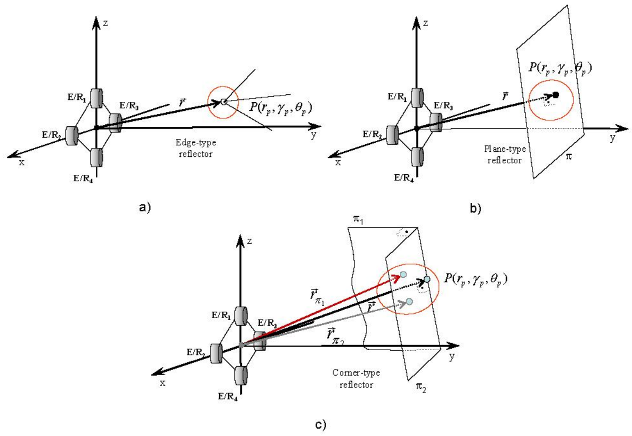

Figure 7. Ultrasonic reflectors considered: a) edge-type, b) plane-type and c) corner-type.

C. Considerated Classes

Before beginning the classification process, it is necessary to remark some considerations associated to the sensorial structure that will be used during the acquisition of the patterns. The emission/reception cone of the sensor is defined by the azimuth angle ($\gamma_{\min} \leq \gamma \leq \gamma_{\max}$) and elevation angle ($\theta_{\min} \leq \theta \leq \theta_{\max}$); and the distance range is defined by $r_{\min}$ and $r_{\max}$. The vector $\vec{r}$, which defines the 3D position of a reflector in the perception zone, is given by their (r, γ, θ) coordinates. The frontal space of the sensorial structure is formed by Q directions defined by (γ_q, θ_q), with $q \in \{1,2,\ldots,Q\}$. Moreover, in every direction q there exist L discrete distances referred as l, with $l \in \{1,2,\ldots,L\}$. The principal goal in this work is to identify a determined reflector located at a direction q and distance l. For that, it is necessary to obtain a set of measurements (or classes) representing every reflector at every q direction and l distance. In Figure 8 the block diagram for the whole classification process is shown. The process begins with the classification of the reflector type, and it subsequently carried out in parallel its localization (direction and distance).

For the classification of the reflector type only three classes are defined, as: $\mathbf{T}^P$, $\mathbf{T}^E$ and $\mathbf{T}^C$ for plane (***P***), edge (***E***) and corner (***C***) reflectors, respectively. Every class is formed by a set of TOF vectors off-line generated. Thus, the specific class of every reflector consists of QxL-TOF vectors, where q possible directions are considered for every distance l.

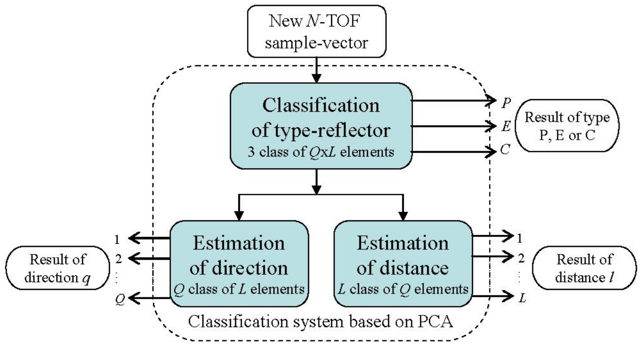

Figure 8. Block diagram of the classification process.

These TOF vectors can be referred as $\mathbf{T}^P = \left[\boldsymbol{\tau}_1^P \;\; \boldsymbol{\tau}_2^P \;\; \cdots \;\; \boldsymbol{\tau}_L^P\right]$ for planes; $\mathbf{T}^E = \left[\boldsymbol{\tau}_1^E \;\; \boldsymbol{\tau}_2^E \;\; \cdots \;\; \boldsymbol{\tau}_L^E\right]$ for edges; and $\mathbf{T}^C = \left[\boldsymbol{\tau}_1^C \;\; \boldsymbol{\tau}_2^C \;\; \cdots \;\; \boldsymbol{\tau}_L^C\right]$ for corners. The TOF vector $\boldsymbol{\tau}_l^\chi$ with q directions and l distances, associated to the χ reflector, can be expressed in generic form as $\boldsymbol{\tau}_l^\chi = \left[\boldsymbol{\tau}_{l,1}^\chi \;\; \boldsymbol{\tau}_{l,2}^\chi \;\; \cdots \;\; \boldsymbol{\tau}_{l,Q}^\chi\right]$, where $\chi \in$ {P, E, C}. Furthermore, the N-dimensional TOF vector $\boldsymbol{\tau}_{l,q}^\chi$ associated to the reflector χ can be expressed as $\boldsymbol{\tau}_{l,q}^\chi = [t_1 \;\; t_2 \;\; \cdots \;\; t_N]^T$; where $\chi \in$ {P, E, C}, $l \in \{1,2,\ldots,L\}$ and $q \in \{1,2,\ldots,Q\}$. When applied the PCA technique, the transformation matrix associated to every class is obtained, referred as $\mathbf{U}^P$, $\mathbf{U}^E$ and $\mathbf{U}^C$ for plane, edge and corner reflectors, respectively. Every matrix has been independently obtained after applying the process explained in (6).

In order to estimate the direction of the reflectors as well as its separation with respect to the sensorial system, the same methodology can be applied. In this classification process, it is necessary to create so many classes as directions are desired to be identified. For that reason, the classes are identified as:

$$\mathbf{T}_q^\chi = \left[\boldsymbol{\tau}_{1,q}^\chi \;\; \boldsymbol{\tau}_{2,q}^\chi \;\; \cdots \;\; \boldsymbol{\tau}_{L,q}^\chi\right] \quad q = 1,2,\ldots,Q \tag{10}$$

Where $\mathbf{T}^\chi_q$ is the class of χ reflector in the q direction and it is characterized by L-TOF vectors to different distances of the sensor. The transformation matrix $\mathbf{U}^\chi_q$ associated to every class is obtained by applying (6), and defined as:

$$\mathbf{U}_q^\chi = \left[\mathbf{u}_{q,1}^\chi \;\; \mathbf{u}_{q,2}^\chi \;\; \cdots \;\; \mathbf{u}_{q,K}^\chi\right] \quad q = 1,2,\ldots,Q \tag{11}$$

Where $\mathbf{U}^\chi_q$ is the optimal transformation matrix in the q direction of the χ reflector; $\mathbf{u}^\chi_{q,k}$ are the more significant K-eigenvectors of the scattering matrix $\mathbf{C}$, with $k \in \{1,2,\ldots,K \mid \forall K \leq N\}$.

In order to estimate the distance of the reflector χ, L new classes associated to each distance l considered are constructed. Every class is defined by:

$$\mathbf{T}_l^\chi = \lfloor \boldsymbol{\tau}_{l,1}^\chi \quad \boldsymbol{\tau}_{l,2}^\chi \quad \cdots \quad \boldsymbol{\tau}_{l,Q}^\chi \rfloor, \quad l = 1,2,\ldots,L \tag{12}$$

Where $\mathbf{T}_l^\chi$ is every class of the reflector χ at the distance l, integrated by Q-TOF vectors corresponding to the different directions from the frontal space. With these classes, the transformation matrices $\mathbf{U}^\chi_l$ associated to every class are obtained by:

$$\mathbf{U}_l^\chi = \lfloor \mathbf{u}_{l,1}^\chi \quad \mathbf{u}_{l,2}^\chi \quad \cdots \quad \mathbf{u}_{l,K}^\chi \rfloor, \quad l = 1,2,\ldots,L \tag{13}$$

Where $\mathbf{U}^\chi_l$ is every optimal transformation matrix associated to the reflector χ at the distance l; and $\mathbf{u}^\chi_{l,k}$ are the more significant K-eigenvectors of the scattering matrix $\mathbf{C}$, where $k \in \{1,2,\ldots,K \mid \forall K \leq N\}$.

D. Strategy of identification and location

After applying the PCA technique to obtain the optimal transformation matrix $\mathbf{U}^\chi_{opt}$, this can be used for the classification process of a new TOF sample-vector $\boldsymbol{\tau}_s$. This new TOF sample-vector can be obtained on-line to carry out a classification in real time. The strategy to identify and locate a reflector in 3D environment is done following the diagram of Figure 8. The first step is to determine the type-reflector of the new sample-vector $\boldsymbol{\tau}_s$ and the second step is to locate its position and distance in parallel, employing the result obtained in the first step. The identification of a reflector χ located at distance r_s and direction q_s starts with its projection to the transformed space by applying (7). The TOF sample-vector $\boldsymbol{\tau}_s$ in the transformed space $\boldsymbol{\rho}^\chi_s$ is determined by:

$$\boldsymbol{\rho}_s^\chi = (\mathbf{U}^\chi)^T \cdot \boldsymbol{\Phi}_s^\chi = (\mathbf{U}^\chi)^T \cdot (\boldsymbol{\tau}_s - \boldsymbol{\Psi}^\chi) \tag{14}$$

With $\boldsymbol{\rho}^\chi_s \in \Re^K$. Next, the sample-vector in the transformed space $\boldsymbol{\rho}^\chi_s$ is recovered by the inverse transformation defined in (8), and the recovered TOF vector $\boldsymbol{\Omega}^\chi_s$ is given by:

$$\boldsymbol{\Omega}_s^\chi = \mathbf{U}^\chi \cdot \boldsymbol{\rho}_s^\chi \tag{15}$$

In this way, the TOF sample-vector $\boldsymbol{\tau}_s$ is projected to the transformed space to estimate its position q_s and distance l_s with respect to the sensor. The sample-vector $\boldsymbol{\tau}_s$ is projected to the transformed space using the optimal transformation matrices in direction $\mathbf{U}^\chi_q$ and distance $\mathbf{U}^\chi_l$; as explained in (16).

$$\boldsymbol{\rho}_{s,q}^\chi = (\mathbf{U}_q^\chi)^T \cdot (\boldsymbol{\tau}_s - \boldsymbol{\Psi}_q^\chi), \quad \boldsymbol{\rho}_{s,l}^\chi = (\mathbf{U}_l^\chi)^T \cdot (\boldsymbol{\tau}_s - \boldsymbol{\Psi}_l^\chi) \tag{16}$$

The sample-vectors $\boldsymbol{\Omega}^\chi_{s,q}$, $\boldsymbol{\Omega}^\chi_{s,l}$ recovered from transformed space are obtained with the inverse transformation defined in (6), as shown in:

$$\boldsymbol{\Omega}_{s,q}^\chi = \mathbf{U}_q^\chi \cdot \boldsymbol{\rho}_{s,q}^\chi, \quad \boldsymbol{\Omega}_{s,l}^\chi = \mathbf{U}_l^\chi \cdot \boldsymbol{\rho}_{s,l}^\chi \tag{17}$$

Finally, the recovery errors (ε_s) are calculated in (9) for every analyzed case (type, position and distance).

$$\begin{aligned} \varepsilon_s^\chi &= \left\| \boldsymbol{\Phi}_s^\chi - \boldsymbol{\Omega}_s^\chi \right\|, \\ \varepsilon_{s,q}^\chi &= \left\| \boldsymbol{\Phi}_{s,q}^\chi - \boldsymbol{\Omega}_{s,q}^\chi \right\|, \\ \varepsilon_{s,l}^\chi &= \left\| \boldsymbol{\Phi}_{s,l}^\chi - \boldsymbol{\Omega}_{s,l}^\chi \right\| \end{aligned} \tag{18}$$

In the type-reflector classification, the belonging of the TOF sample-vector $\boldsymbol{\tau}_s$ to any class associated to only one transformation matrix is determined by means of the smallest recovery error calculated. For example, for a plane identification the recovery error ε^P_s should be smaller than others ($\varepsilon^P_s < \varepsilon^E_s \wedge \varepsilon^P_s < \varepsilon^C_s$). After the reflector identification, the estimation of the position q_s and distance l_s can be determined in the same way, following a similar procedure. To estimate the direction q_s, the sample-vector $\boldsymbol{\tau}_s$ is compared to all possible q directions and the smallest recovery error obtained ε^χ_{s,q_s} corresponds to the position of the identified reflector ($\varepsilon^\chi_{s,q_s} < \varepsilon^\chi_{s,q}$). The distance is estimated by comparing the TOF sample-vector $\boldsymbol{\tau}_s$ with all distance classes T^χ_l, and the smallest recovered error ε^χ_{s,l_s} is associated to the corresponding distance l_s ($\varepsilon^\chi_{s,l_s} < \varepsilon^\chi_{s,l}$).

IV. Classification and Estimation Results

In order to verify the effectiveness of the classification system of ultrasonic reflectors based on PCA technique, some tests have been carried out using data generated by a TOF simulator. Every 3D reflector characterized in previous Section has been used as reference in the simulator to obtain the training set of TOF vectors. Every reflector has been placed at different positions q and distances l, considering the map of directions from Section II. Every direction q is defined by the γ azimuth and θ elevation angles. The reflectors were gradually placed, starting from 50cm until 310cm, at intervals of 20cm. In Figure 4 are shown the Q (Q=61) possible directions considered at every distance l.

New TOF sample-vectors different from the training set have been obtained in order to test the classification system. In that way, intermediate measurements have been chosen, so the system can discriminate an object outside the reference values. The distance measurements used in the test, considering the three reflector types in the Q directions, are {40cm, 52cm, 87cm, 133cm, 160cm, 202cm, 249cm}. Table II shows the results obtained by the classification system based on PCA technique, identifying and locating a 3D reflector. The tests were carry out with data not included in the training patterns, considering that every sample-vector contains a Gaussian noise of 5 μs.

TABLE II

Success percentage in the classification of a plane-type reflector.

Reflector	*Success in the Identification*	*Directions* estimated (61/61)*	*Distances estimated (7/7)*
Plane	98%	100%	100%
Edge	95%	100%	100%
Corner	96%	100%	100%

*Considering the measurements test in the Q directions

In order to obtain a success classification applying the PCA technique, the optimal transformation matrices of each reflector were generated by using only 3 eigenvectors. In Figure 9 the correct identification of the plane-type reflector is shown, considering the Q possible directions at the distance 160cm and a Gaussian noise of 5 µs. The classification system shows that the algorithm is more efficient in the centre of the direction map, although the reflector type can be always identified.

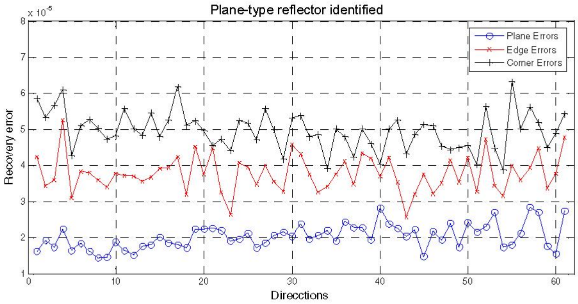

Figure 9. Classification of a plane-type reflector placed at 1.6m.

Figure 10 shows the identification of the edge-type and corner-type reflectors with the classification system, independently on position in the 3D environment. In this process classification all the possible Q directions of the direction map are included.

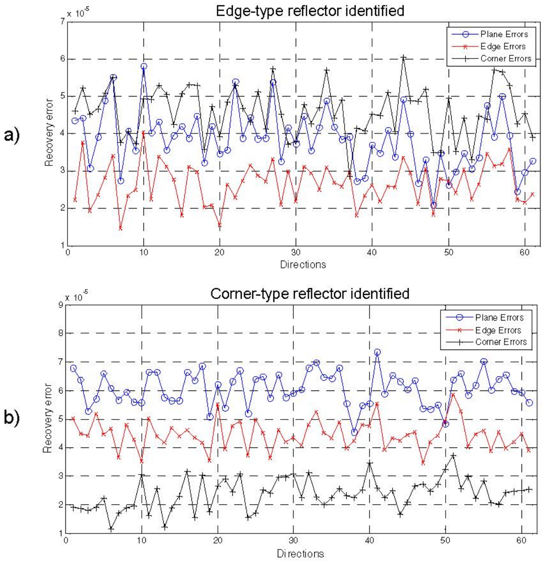

Figure 10. Identification of the reflector with the classification system. a) Edge-type reflector and b) Corner-type reflector.

In Figure 11 the correct estimation of the distance l_s and direction q_s is shown for a plane-type reflector located at 133 cm and in the position 35 of the direction map. It is observed that there are other near positions with local minimum error together with the smallest error (position 18 and 58 of direction map).

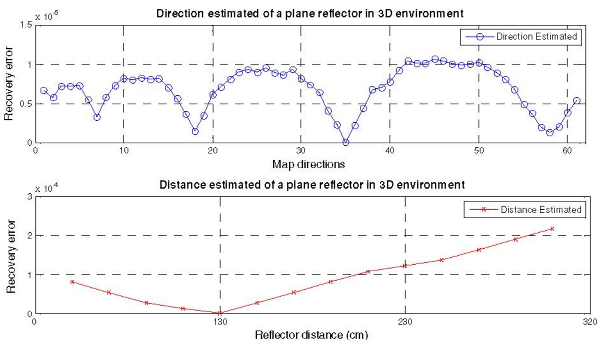

Figure 11. Estimation of the direction and distance for a plane-type reflector.

V. Conclusions

In this work a classification system based on PCA technique for the recognition of reflectors in three-dimensional (3D) environments is presented. With this classification system it is possible to discriminate among three types of basic three-dimensional reflectors: planes, corners and edges.

The obtained results show the feasibility of the proposal with satisfactory classification and location of the object. The classification system uses a vector formed by 16 TOFs determined by the sensorial system. In addition to the type reflector classification, this classification system is able to accurately estimate the position of the reflector (direction and distance).

Acknowledgment

This work has been possible thanks to the Madrid Community (INCUBUS: CCG06-UAH/DPI-0725), from the Spanish Ministry of Science and Technology (RESELAI: TIN2006-14986-CO2-01) and Spanish Ministry of Promotion (VIATOR: ref 70025-T05).

References

[1] H. Peremans, K. Audenaert, J.M. Van Campenhout. "A high-resolution sensor based on tri-aural perception". IEEE Transactions on Robotics and Automation, Vol. 9, Nº. 1, page(s): 36-48, February 1993.

[2] B. Barshan, R. Kuc. "Differentiating sonar reflections from corners and planes by employing an intelligent sensor". IEEE Transactions on Pattern Analysis and Machine Intelligence, Vol. 12, Issue 6, June 1990. Page(s):560 – 569.

[3] B. Ayrulu, B. Barshan, S.W. Utete. "Target identification with multiple logical sonars using evidential reasoning and simple majority voting". IEEE International Conference on Robotics and Automation, Vol. 3, 20-25 April 1997. Page(s):2063–2068.

[4] J. Ureña, M. Mazo, J.J. García, A. Hernández, E. Bueno. "Classification of reflectors with an ultrasonic sensor for mobile robots applications". Robotics and Autonomous Systems. Vol. 29, December 1999. Page(s): 269 – 279.

[5] Xianbin Wang, Y. Wu, B. Caron, "Transmitter identification using embedded pseudo random sequences", IEEE Transactions on Broadcasting, Vol. 50, Issue 3, Sept. 2004 Page(s):244–252.

[6] C. De Marziani, J. Ureña, A. Hernández, M. Mazo, F. Álvarez, J. García, P. Donato. "Modular Architecture for Efficient Generation and Correlation of Complementary Set of Sequences". IEEE Transactions on Signal Processing, Vol. 55, Issue 5, Part 2, May 2007 Page(s):2323 – 2337.

[7] M.L. Hong, L. Kleeman. "A low sample rate 3D sonar sensor for mobile robots". IEEE International Conference on Robotics and Automation. Vol. 3, 21-27 May 1995. Page(s): 3015 – 3020.

[8] J. Yang, D. Zhang, A. F. Frangi, J. Yang. "Two-Dimensional PCA: a New Approach to Appearance-Based Face Representation and Recognition". IEEE Transactions on Pattern Analysis and Machine Intelligence, Vol. 26, No. 1, Page(s): 131-137, January 2004.

[9] J.A. Jiménez, J. Ureña, M. Mazo, A. Hernández, E. Santiso. "Using PCA in Time-of-Flight Vectors for Reflectors Recognition and 3-D Localization". IEEE Transactions on Robotics, Vol. 21, No. 5, October 2005. Page(s): 909 – 924.